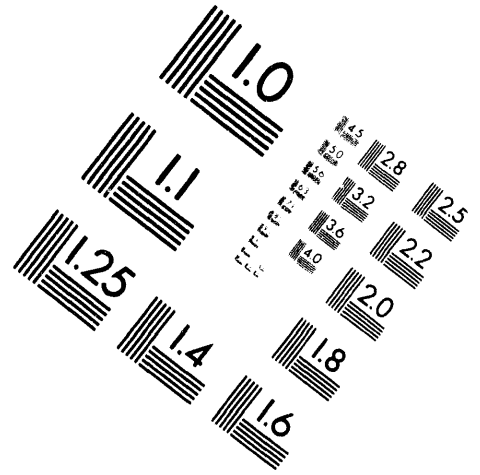
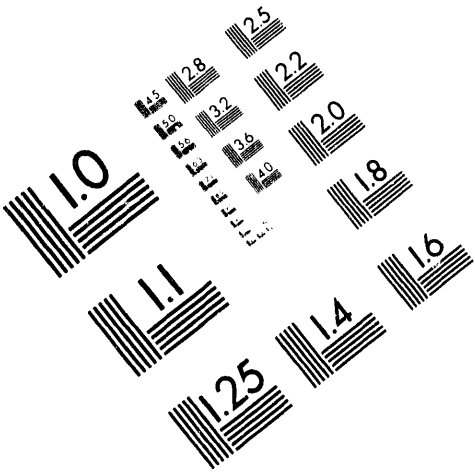




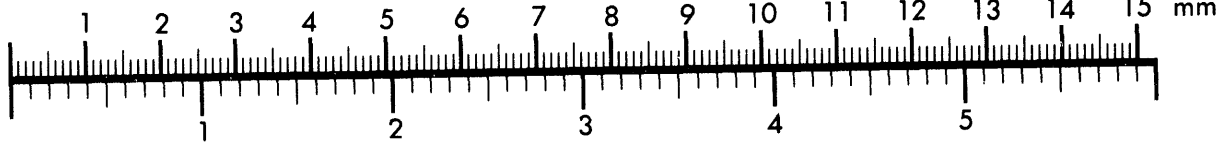
**AIM**

**Association for Information and Image Management**

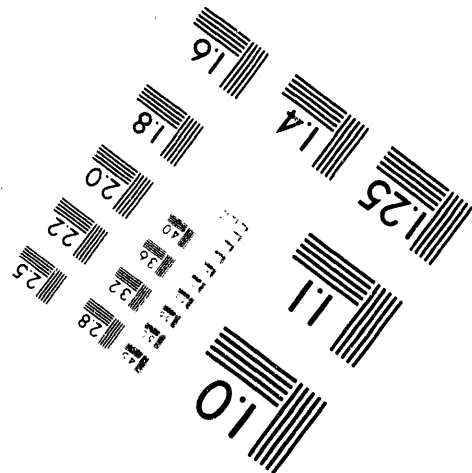
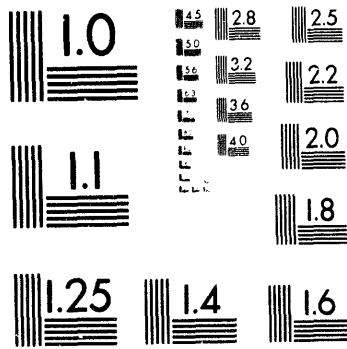
1100 Wayne Avenue, Suite 1100  
Silver Spring, Maryland 20910  
301/587-8202



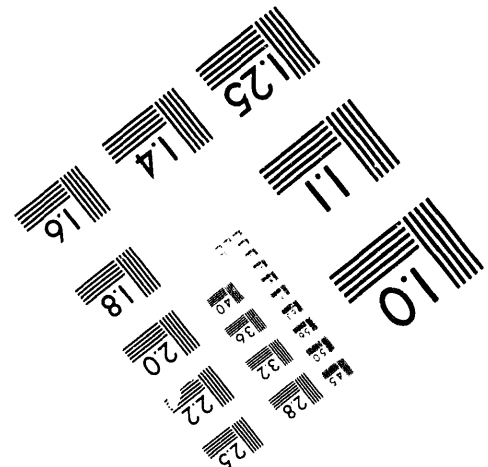
Centimeter



Inches



MANUFACTURED TO AIM STANDARDS  
BY APPLIED IMAGE, INC.



**1 of 1**

Conf-931115-4

[Note: This is a preprint of a document submitted for publication. Contents of this document should not be quoted or referred to without permission of the author(s).]

To be presented at the Symposium on the Science of Advanced Batteries, Cleveland, Ohio, November 8-9, 1993 and published in *Proceedings*

### THIN-FILM RECHARGEABLE LITHIUM BATTERIES

J. B. Bates, G. R. Gruzalski, N. J. Dudney, C. F. Luck, Xiaohua Yu  
Oak Ridge National Laboratory  
Oak Ridge, Tennessee 37831-6030

"The submitted manuscript has been authored by a contractor of the U.S. Government under contract No. DE-AC05-84OR21400. Accordingly, the U.S. Government retains a nonexclusive, royalty-free license to publish or reproduce the published form of this contribution, or allow others to do so, for U.S. Government purposes."

#### DISCLAIMER

This report was prepared as an account of work sponsored by an agency of the United States Government. Neither the United States Government nor any agency thereof, nor any of their employees, makes any warranty, express or implied, or assumes any legal liability or responsibility for the accuracy, completeness, or usefulness of any information, apparatus, product, or process disclosed, or represents that its use would not infringe privately owned rights. Reference herein to any specific commercial product, process, or service by trade name, trademark, manufacturer, or otherwise does not necessarily constitute or imply its endorsement, recommendation, or favoring by the United States Government or any agency thereof. The views and opinions of authors expressed herein do not necessarily state or reflect those of the United States Government or any agency thereof.

SOLID STATE DIVISION  
OAK RIDGE NATIONAL LABORATORY  
Managed by  
MARTIN MARIETTA ENERGY SYSTEMS, INC.  
under  
Contract No. DE-AC05-84OR21400  
with the  
U.S. DEPARTMENT OF ENERGY  
Oak Ridge, Tennessee 37831-6030

November 1993

MASTER  
DISTRIBUTION OF THIS DOCUMENT IS UNLIMITED *gtd*

## THIN-FILM RECHARGEABLE LITHIUM BATTERIES

J. B. Bates, G. R. Gruzalski, N. J. Dudney, C. F. Luck, Xiaohua Yu  
Oak Ridge National Laboratory  
Oak Ridge, Tennessee 37831-6030

### Abstract

Rechargeable thin-film batteries with lithium metal anodes, an amorphous inorganic electrolyte, and cathodes of lithium intercalation compounds have been fabricated and characterized. The cathodes include  $\text{TiS}_2$ , the  $\omega$  phase of  $\text{V}_2\text{O}_5$ , and the cubic spinel  $\text{Li}_x\text{Mn}_2\text{O}_4$  with open circuit voltages at full charge of about 2.5 V, 3.7 V, and 4.2 V, respectively. The development of these robust cells, which can be cycled thousands of times, was possible because of the stability of the amorphous lithium electrolyte, lithium phosphorus oxynitride. This material has a typical composition of  $\text{Li}_{2.9}\text{PO}_{3.3}\text{N}_{0.46}$  and a conductivity at 25°C of 2  $\mu\text{S}/\text{cm}$ . Thin-film cells have been cycled at 100% depth of discharge using current densities of 2 to 100  $\mu\text{A}/\text{cm}^2$ . The polarization resistance of the cells is due to the slow insertion rate of  $\text{Li}^+$  ions into the cathode. Chemical diffusion coefficients for  $\text{Li}^+$  ions in the three types of cathodes have been estimated from the analysis of ac impedance measurements.

### Introduction

The fabrication of a rechargeable thin-film lithium battery was first reported in 1983 by Kanehori and co-workers [1]. The cells, consisting of a lithium anode, an amorphous  $\text{Li}_{3.6}\text{Si}_{0.6}\text{P}_{0.4}\text{O}_4$  electrolyte, and a  $\text{TiS}_2$  cathode, were cycled several thousand times at current densities up to 16  $\mu\text{A}/\text{cm}^2$ . Levasseur and colleagues [2] fabricated rechargeable thin-film lithium cells using a titanium oxysulfide cathode, a  $\text{Li}_2\text{O}-\text{B}_2\text{O}_3-\text{Li}_2\text{SO}_4$  electrolyte, and a lithium anode [3]. Up to 50 cycles were reported at current densities as high as 62  $\mu\text{A}/\text{cm}^2$ . At about the same time, Creus et al. described [4] the fabrication of thin-film lithium batteries using amorphous  $\text{V}_2\text{O}_5$ - $\text{TeO}_2$  cathodes, amorphous lithium silicon-phosphorus sulfide electrolytes, and lithium anodes. The initial poor performance of the cells due to reaction of Li with

the electrolyte was improved by adding a layer of LiI between the electrolyte and the lithium anode.

The technique of protecting the electrolyte with a layer of LiI deposited between the electrolyte film and the anode film was successfully used by Jones and colleagues at Eveready Battery Co. [4,5] to develop thin-film Li-TiS<sub>2</sub> batteries with excellent performance over thousands of charge-discharge cycles. Several of the Eveready cells have undergone more than 10,000 cycles at current densities of up to 100  $\mu\text{A}/\text{cm}^2$  with little change in performance, while others stored at room temperature for nearly two years have retained 98% of their initial voltage. However, the LiI layer limits the cathodes which can be used due its restricted stability window of about 2.8 V [6], and it further complicates cell fabrication. Recently, we reported the discovery [7,8] of a new lithium electrolyte, lithium phosphorus oxynitride, that is stable at high-cell potentials, and thin-film rechargeable lithium batteries having open circuit voltages ranging from 4.2 to 2.5 V using Li<sub>x</sub>Mn<sub>2</sub>O<sub>4</sub>, V<sub>2</sub>O<sub>5</sub>, and TiS<sub>2</sub> cathodes, respectively, have been fabricated [9]. In addition, some success has been achieved in protecting the lithium anode with a thin-film coating so that cells have been able to survive for several months in air. In this paper, we discuss the fabrication and characterization of thin-film lithium batteries with emphasis on the Li-V<sub>2</sub>O<sub>5</sub> system.

### Cell Fabrication and Characterization

A cross-sectional drawing of a typical thin-film battery is shown in Fig. 1. The cathode illustrated is vanadium pentoxide (V<sub>2</sub>O<sub>5</sub>), but it could be any one of several lithium intercalation compounds that can be deposited in thin-film form. The steps for the fabrication of a Li-V<sub>2</sub>O<sub>5</sub> cell illustrated in Fig. 2 are listed in Table 1. For the sputter depositions, two-inch magnetrons (Torus) were used. The cathode and

electrolyte films were deposited at rates of about  $0.1 \mu\text{m/hr}$  to thicknesses of typically  $0.5$  to  $1 \mu\text{m}$ . A variety of techniques have been used to characterize the physical and chemical properties of individual cathode and electrolyte films [10,11]. The lithium films were deposited at a rate of about  $10 \mu\text{m/hr}$  by evaporation of lithium metal contained in a Ti crucible. Typically  $3$ - to  $5\text{-}\mu\text{m}$  thick films were deposited corresponding to five to ten times more lithium required for the full capacity of the cathode films. After the lithium deposition, the cells were transferred in Ar to another deposition system where the protective coating was applied. Cells based on  $\text{TiS}_2$  and  $\text{LiMn}_2\text{O}_4$  were fabricated in a similar manner using cathodes prepared elsewhere by methods described in the literature [4,5,12].

The thin-film cells typically have an area of about  $1 \text{ cm}^2$  and are about  $6\text{-}\mu\text{m}$  thick (uncoated), and they are usually deposited on  $1$ " square glass microscope slides. Recently cells with an area of about  $4 \text{ cm}^2$  were deposited onto alumina substrates. For cells based on  $\text{V}_2\text{O}_5$  or  $\text{TiS}_2$  cathodes, all depositions are carried out at ambient temperature, so these batteries could be fabricated on virtually any substrate capable of supporting a thin film. For example,  $\text{Li-V}_2\text{O}_5$  cells have been fabricated on alumina, glass, and  $0.1\text{-mm}$ -thick polyester. The  $\text{LiMn}_2\text{O}_4$  cathode, however, requires [12] a post deposition anneal of about  $400^\circ\text{C}$  in order to obtain the crystalline spinel phase. Consequently, until a lower temperature deposition process can be found, the selection of substrates onto which  $\text{Li-LiMn}_2\text{O}_4$  batteries can be fabricated is limited.

Cycling of the thin-film cells at constant current between specified voltage limits was carried out using two Keithley 617 electrometers operated under computer control. At the end of each half-cycle, the voltage was held constant until the current decreased to a specified fraction of the charge or discharge current, usually  $10\%$ . Recently cell testing has also been performed on a modified Maccor Series 2000 Battery Test System. The impedance of the cells at different potentials

was measured at 25°C at frequencies from 0.01 Hz to 10 MHz [13]. A dc bias equal to the OCV was applied to the cells during the impedance measurements, and the ac voltage was 50 mV or less. The OCV measured before and after the impedance measurements agreed within a few mV.

## Results and Discussion

### *Electrolyte*

The good performance of the thin-film rechargeable lithium batteries discussed below can be attributed to the electrolyte, an amorphous lithium phosphorus oxynitride, denoted by Lipon. This material [7,8] that has a lithium ion conductivity of about  $2 \times 10^{-6}$  S/cm at 25°C, a  $\text{Li}^+$  transport number of unity, and, most importantly, is stable in contact with metallic Li at high-cell voltages. Recent I-V measurements on V/Lipon/V thin-film structures indicate that the decomposition voltage of Lipon is about 5.5 volts. The composition of Lipon, as determined from Rutherford backscattering spectrometry (RBS) and proton induced gamma ray emission (PIGE) analysis [8], is typically  $\text{Li}_{2.9}\text{PO}_{3.3}\text{N}_{0.46}$ , but the N content has been observed to vary from 2 to 6 at. %.

### *V<sub>2</sub>O<sub>5</sub>*

The phase and microstructure of vanadium oxide films deposited by reactive dc magnetron sputtering of V in Ar + O<sub>2</sub> are sensitive to several process variables including substrate temperature, substrate bias, and process gas composition. The preferred form for thin-film batteries is a smooth, apparently x-ray amorphous structure that is evidently the same as the disordered crystalline  $\omega$ -V<sub>2</sub>O<sub>5</sub> investigated in bulk form by Delmas et al. [13]. The O/V ratios of these films determined from RBS and Auger measurements agree well: O/V =  $2.5 \pm 0.1$ . The density of the films has not been accurately determined, but from measurements of film thickness

(using a profilometer) and mass (obtained from deposition rates determined with a quartz crystal oscillator), an average density of  $3 \text{ g/cm}^3$  was obtained from six separate depositions. Kennedy et al. [14] reported that the density of  $\text{V}_2\text{O}_5$  films grown by evaporation ranged from  $2.42 \text{ g/cm}^3$  to  $2.69 \text{ g/cm}^3$ . We measured the electronic conductivity of a  $\text{V}_2\text{O}_5$  film sandwiched between V contacts to be  $1.5 \times 10^{-7} \text{ S/cm}$  at  $25^\circ\text{C}$ , considerably smaller than the values of  $10^{-6} \text{ S/cm}$  reported for the evaporated thin films [14] and of  $4 \times 10^{-5} \text{ S/cm}$  for amorphous  $\text{V}_2\text{O}_5$  films deposited by sputtering vanadium oxide targets [15].

Examples of charge-discharge curves for Li- $\text{V}_2\text{O}_5$  cells are illustrated in Figs. 3. The Li- $\text{V}_2\text{O}_5$  cells are deposited in the fully charged state. Based upon the mass of the films estimated from the deposition rate, the first deep discharge of these cells to 1.5 V is represented



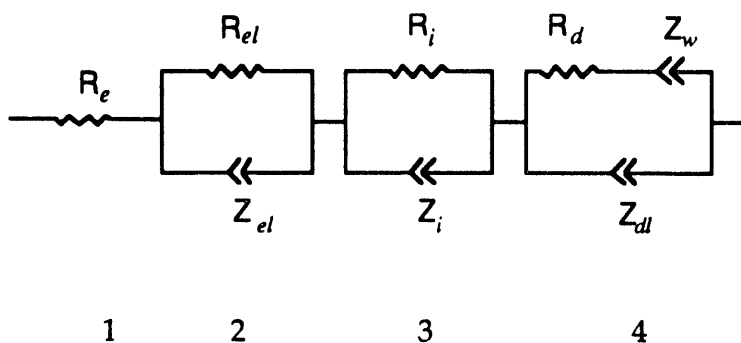
in agreement with results obtained with bulk  $\omega$ - $\text{V}_2\text{O}_5$  [13]. On the subsequent charge cycle, about 2.8 Li per  $\text{V}_2\text{O}_5$  is extracted from the cathode. A comparable capacity loss on the first discharge is also observed when the lower cutoff voltage is 2.7 V as illustrated in Fig. 3(a). It can be seen in this figure that the quantity of charge passed through the cell on the first discharge is larger than that of the following cycles. This initial large loss in capacity is not understood, but it has been suggested [16,17] that a discharge below about 2 Li per  $\text{V}_2\text{O}_5$  in crystalline vanadium oxide induces an irreversible formation of domains with deep potential wells that trap lithium ions which are not extracted on subsequent charge cycles. As illustrated in Fig. 4, after the first discharge, there is a slow but continuous decrease in the amount of lithium inserted into (and extracted from) the cathode, possibly due to further irreversible structural changes. For cycling to 1.5 V, this capacity loss reaches a level rate of about



0.6% per cycle. For one of the cells, this loss was reduced to about 0.1% when the lower cutoff voltage was increased to 1.8 V.

In addition to the gradual decrease in the charge cycled through the cell, the charge extracted or inserted on each half cycle often oscillates about a monotonic decreasing function, as shown by the data from cell 61A in Fig. 4. The cause of this oscillation is not understood, but it might be related to the failure to reach equilibrium in the cathode before the next half cycle begins.

The results of discharging a cell to a constant capacity using different current densities shown in Fig. 5 illustrate the effect of polarization resistance. The current densities of 2, 5, 10, 20, 40, and 100  $\mu\text{A}/\text{cm}^2$  correspond to C rates of 0.04, 0.08, 0.19, 0.38, 0.77 and 1.9, respectively. From the evidence accumulated to date, the polarization resistance of all of the thin film cells we have investigated, including the those with  $\text{Li}_x\text{Mn}_2\text{O}_4$  and  $\text{TiS}_2$  cathodes, is due mainly to the slow rate of insertion of  $\text{Li}^+$  ions into the cathode. Examples of the impedance spectra for two  $\text{Li-V}_2\text{O}_5$  cells are shown in Fig. 6. The solid curves were obtained by a fit of the equivalent circuit model shown below to the impedance data. The model is constructed from the four components labeled 1-4. The constant phase angle (CPA) elements  $Z$  in the



circuit have the form  $Z = A(j\omega)^{-n}$ , where  $A$  and  $n$  are constants [18]. Components 1, 2, and 4 represent the electronic resistance of the cathode, the impedance of the electrolyte, and the impedance of the cathode, respectively. The latter was assumed to have the form similar to Randles [19]. In this model,  $R_d$  is usually called the charge transfer resistance,  $Z_w$  the diffusion impedance, and  $Z_{dl}$  the impedance of the double layer at the cathode-electrolyte interface. For  $Z_{el}$ ,  $Z_i$ , and  $Z_{dl}$ , the frequency exponent  $n$  is on the order of 0.8. For the Warburg term,  $Z_w$ ,  $n = 1/2$ . The origin of component 3 in the model is not known at this time, but it is associated with the formation of the Lipon- $V_2O_5$  interface. All four of the equivalent circuit components also appear in the impedance spectra of a V/Lipon/ $V_2O_5$ /V thin-film structure, so component 3 is not due to the Li-electrolyte interface. Moreover, this component does not appear in the impedance spectra of a Li- $Li_xMn_2O_4$  cell nor that of a Li- $TiS_2$  cell.

Ho et al. [20] extended Randles' model to intercalation cathodes and obtained a relationship between the constant  $A_w$  and the chemical diffusion coefficient  $\tilde{D}_i$  for the cations in the cathode:

$$A_w = \frac{V_m dV/dx}{\sqrt{2} Fa} \cdot \frac{1}{\sqrt{\tilde{D}_i}} \quad (2)$$

where  $dV/dx$  is the derivative of the cell potential with the change in the cation stoichiometry parameter, e.g.,  $x$  in  $Li_xV_2O_5$ ,  $V_m$  is the molar volume,  $F$  is Faraday's constant, and  $a$  is the area of the cathode. The diffusion coefficients given in Table 2 were calculated by from Eq. (2) using the fitted values of  $A_w$ ,  $V_m = 54.1 \text{ cm}^3/\text{mol}$  (crystalline value), and  $dV/dx = 0.75 \text{ V}$ . These are effective diffusion coefficients which include not only the ionic mobility and thermodynamic enhancement factors but also the film microstructure. By comparison, Baudry et al. [21] reported a diffu-

sion coefficient of  $2.5 \times 10^{-12}$  cm<sup>2</sup>/s for Li<sup>+</sup> ions in V<sub>2</sub>O<sub>5</sub> thin films grown by evaporation as determined from impedance measurements on an electrochromic window at 3V/Li.

The term  $R_d$  in the Randles circuit is usually referred to as a charge transfer resistance implying both ionic and electronic contributions. In the cells we have investigated, the magnitude of  $R_d$  arises solely from the resistance to insertion of Li<sup>+</sup> ions into the cathode with no evident contribution from electron transport. The magnitude of  $R_d$  is largest in the fully charged cell and decreases as Li is added to the cathode. The decrease in  $R_d$  is accompanied by a decrease in the Warburg parameter,  $A_w$ . The decrease in both of these parameters is due the increase in lithium ion mobility in the cathode with lithium insertion.

#### *Li<sub>x</sub>Mn<sub>2</sub>O<sub>4</sub>*

Examples of the charge-discharge curves for a Li-LiMn<sub>2</sub>O<sub>4</sub> cell are shown in Fig. 7. The as-deposited cathode has a composition near LiMn<sub>2</sub>O<sub>4</sub> [12], but the open circuit voltage of a cell can vary between 3 and 3.9 V depending on the exact lithium content. The battery is first charged to 4.5 V. Assuming that one Li per Mn<sub>2</sub>O<sub>4</sub> is extracted from the cathode during this initial charge [12], the subsequent discharge-charge cycles, restricted to the voltage range shown in Fig. 7, should be represented by



However, compared to the amount of cathode deposited, about 0.6 Li per Mn<sub>2</sub>O<sub>4</sub> is cycled through the cell after the initial charge. Possibly the estimated mass of the cathode was too large, but in any case it appears that a significant fraction of the as-deposited cathode becomes "electrochemically inactive" after the initial charge. This suggests an irreversible structural change occurs in the cathode on the initial charge.

A continuous subtle structural change with cycling is indicated by the data in Fig. 8. After the first charge, the amount of lithium that can be inserted into the cathode continues to decrease by about 0.1% on each successive cycle. The oscillatory behavior observed with  $V_2O_5$  is seen in this case as well. Impedance measurements on the  $Li-Li_xMn_2O_4$  cell also showed that the polarization resistance is dominated by slow lithium insertion into the cathode, but the resistance was an order of magnitude lower than that of the  $V_2O_5$  cathodes. The chemical diffusion coefficient for  $Li^+$  in the cathode calculated from the Warburg coefficient  $A_w$  was  $3 \times 10^{-12} \text{ cm}^2/\text{s}$ .

The charge-discharge curves (Fig. 7) are well-behaved provided the lower voltage cutoff does not fall below about 3.6 V. If the discharge is extended beyond the cathode composition of  $LiMn_2O_4$  (i.e.,  $Li_{1+x}Mn_2O_4$ ), the cell potential drops abruptly to 3 V, indicating the appearance of a second phase. When the discharge voltage was reduced to 3 V after completing 150 cycles of the  $Li-Li_xMn_2O_4$  cell, the films detached from the substrate, possibly due to the nearly 6% increase in unit cell volume that occurs during the phase change [22].

### $TiS_2$

Several cells were fabricated using  $TiS_2$  cathodes prepared by S. Jones of Eveready Battery Co. As with the  $V_2O_5$  and  $Li_xMn_2O_4$  cathodes, impedance measurements of the cells at several discharge states show that the polarization resistance is dominated by the slow insertion of  $Li^+$  ions into the  $TiS_2$  lattice. One of the cells underwent 4025 deep cycles at current densities from 5 to  $100 \mu\text{A}/\text{cm}^2$  before failing in short circuit. The cell was fractured by scoring the glass substrate and examined in a scanning electron microscope. The micrograph of a cross section shown in Fig. 9 illustrates clearly that interface between the lithium anode and the Lipon electrolyte remained sharp and smooth at least on a submicron scale. The

absence of any dendrite growth is consistent with our observations and those of Jones et al. that, except for the gradual capacity loss, there is virtually no change in the charge-discharge curves after many cycles of thin film lithium cells.

The energy densities, specific energies, and capacities for the Li-TiS<sub>2</sub>, Li-V<sub>2</sub>O<sub>5</sub>, and Li-Li<sub>x</sub>Mn<sub>2</sub>O<sub>4</sub> thin-film batteries are listed in Table 3. The energy of the cells was determined from the integrals  $\int V(q)dq$  over the respective discharge curves calculated between the voltages specified in the second column in the table. The mass and volume of the cells were based on 1- $\mu$ m-thick cathode and electrolyte films plus an anode film thick enough to provide three times the maximum amount of Li required by the respective cathodes assuming discharge compositions LiTiS<sub>2</sub>, Li<sub>3</sub>V<sub>2</sub>O<sub>5</sub>, and LiMn<sub>2</sub>O<sub>4</sub>. For the cathodes, the crystalline densities were assumed, although the actual densities of the TiS<sub>2</sub> and V<sub>2</sub>O<sub>5</sub> films are lower. This procedure was followed because the density of the LiMn<sub>2</sub>O<sub>4</sub> film has not been determined. For the electrolyte film, the density of 2.4 g/cm<sup>3</sup> reported [23] for a bulk lithium phosphorus oxynitride glass was assumed. If the actual film densities for V<sub>2</sub>O<sub>5</sub> and TiS<sub>2</sub> were used, the energy densities would be reduced by about 10%.

### Conclusions

The rechargeable thin-film lithium batteries described in this paper have high specific energies and energy densities, the ability to undergo thousands of charge-discharge cycles, and they can be fabricated into a variety of sizes and shapes on virtually any type of substrate. At the present time, the useful current that can be supplied by these cells is limited to 100  $\mu$ A or less per cm<sup>2</sup> of cathode area at room temperature due to the slow rate of insertion of Li<sup>+</sup> ions into the cathodes. Possible methods for improving the insertion rate will be emphasized in future research.

### Acknowledgments

The authors wish to thank Mr. Steve Jones of Eveready Battery Co. for providing several of the  $\text{TiS}_2$  cathodes and for the long cycling of a Li-TiS<sub>2</sub> cell with the Lipon electrolyte. We also thank Dr. F. Shokoohi of Belcore for supplying a thin-film of  $\text{LiMn}_2\text{O}_4$  that we used in fabricating the Li-Li<sub>x</sub>Mn<sub>2</sub>O<sub>4</sub> battery. This research was sponsored by the U.S. Department of Energy Division of Materials Sciences, Office of Transportation Technologies, Division of Chemical Sciences, and Office of Energy Research Technology Transfer Program under contract DE-AC05-84OR21400 with Martin Marietta Energy Systems, Inc.

### References

1. K. Kanehori, K. Matsumoto, K. Miyauchi, and T. Kudo, *Solid State Ionics*, 9&10, 1445 (1983).
2. G. Meunier, R. Dormoy, and A. Levasseur, *Mater. Sci. and Eng. B3*, 19 (1989).
3. R. Creus, J. Sarradin, R. Astier, A. Pradel, and M. Ribes, *ibid.*, B3, 109 (1989).
4. S. D. Jones, J. R. Akridge, S. G. Humphrey, C.-C. Liu, and J. Sarradin, p. 31, *MRS Symposium Proceedings*, Vol. 210, edited by G.-A. Nazri, D. F. Shriver, R. A. Huggins, and M. Bulkanski, Materials Research Society, Pittsburgh, Pennsylvania, 1990.
5. S. D. Jones and J. R. Akridge, *J. Power Sources*, 43-44, 505 (1993).
6. R. A. Huggins in *Proceedings of the Symposium on Lithium Batteries*, ed. by A. N. Dey (The Electrochemical Society, Pennington, NJ, 1987), Vol 87-1, p. 356.
7. J. B. Bates, G. R. Gruzalski, N. J. Dudney, and C. F. Luck, p. 337, *Proc. 35th Power Sources Symposium* (1992).
8. J. B. Bates, N. J. Dudney, G. R. Gruzalski, R. A. Zuhr, A. Choudhury, C. F. Luck, and J. D. Robertson, *J. Power Sources*, 43-44, 103 (1993).
9. J. B. Bates, G. R. Gruzalski, N. J. Dudney, C. F. Luck, X.-H. Yu, and S. D. Jones, *Solid State Technology*, 36, 59 (1993).

10. J. B. Bates, N. J. Dudney, C. F. Luck, B. Sales, and R. Zuhr, *J. Am. Ceram. Soc.*, 74, 929 (1993).
11. J. B. Bates, N. J. Dudney, G. R. Gruzalski, R. A. Zuhr, A. Choudhury, C. F. Luck, and J. D. Robertson, *Solid State Ionics*, 53-56, 647 (1992).
12. F. K. Shokoohi, J. M. Tarascon, B. J. Wilkens, D. Guyomard, and C. C. Chang, *J. Electrochem. Soc.*, 139, 1845 (1992).
13. C. Delmas, S. Brethes, and M. Menetrier, *J. Power Sources* 34, 113 (1991).
14. T. N. Kennedy, R. Hakim and J. D. Mackenzie, *Mat. Res. Bull.*, 2, 193 (1967).
15. F. P. Koffyberg and F. A. Benko, *Phil. Mag.* 38, 357 (1978).
16. S. Hub, A. Tranchant, and R. Messina, *Electrochem. Acta*, 33, 997 (1988).
17. C. A. Cartier, A. Tranchant, M. Verdaguer, R. Messina, and H. Dexpert, *Electrochem. Acta*, 35, 889 (1990).
18. J. B. Bates, J.C. Wang, and Y. T. Chu, *J. Non-Cryst. Solids* 131-133, 1046 (1991).
19. J. E. B. Randles, *Disc. Faraday Soc.* 1, 11 (1947).
20. C. Ho, I. D. Raistrick, and R. A. Huggins, *J. Electrochem. Soc.* 127, 343 (1980).
21. P. Baudry, M. A. Aegerter, D. Deroo, and B. Valla, *J. Electrochem. Soc.* 138, 460 (1991).
22. T. Ohzuku, M. Kitagawa, and T. Hirai, *J. Electrochem. Soc.*, 137, 769 (1990)
23. L. Boukbir and R. Marchand, *Rev. Chim. Min.*, 23, 343 (1986).

Table 1. Steps in the fabrication of thin-film lithium batteries illustrated in Fig. 1b.

- 
1. V current collectors—dc magnetron sputtering of V in Ar
  2.  $V_2O_5$  cathode—dc magnetron sputtering of V in Ar + 14%  $O_2$
  3. Li electrolyte—rf magnetron sputtering of  $Li_3PO_4$  in  $N_2$
  4. Li anode—evaporation of Li ( $10^{-6}$  Torr)
  5. Protective coating
-



Table 2. Chemical diffusion coefficients  $\tilde{D}_{\text{Li}}$  for  $\text{Li}^+$  ions in  $\text{V}_2\text{O}_5$  cathodes as a function of Li content:  $\text{Li}_x\text{V}_2\text{O}_5$

$\text{Li}_x\text{V}_2\text{O}_5$					
Cell 76A			Cell 199A		
$V_o(\text{V})$	$x$	$\tilde{D}_{\text{Li}}(\text{cm}^2/\text{s})$	$V_o(\text{V})$	$x$	$\tilde{D}_{\text{Li}}(\text{cm}^2/\text{s})$
3.4	0.29	$4 \times 10^{-15}$	3.5	0.14	$2.7 \times 10^{-14}$
2.6	1.4	$2.6 \times 10^{-13}$	2.6	1.4	$1.3 \times 10^{-12}$
1.8	2.6	$2.6 \times 10^{-12}$	1.6	2.9	$1.6 \times 10^{-12}$

$$V_m = 54.1 \text{ mol/cm}^3, dV/dx = 0.75\text{V}$$

Table 3. Comparison of three types of rechargeable thin-film lithium batteries.

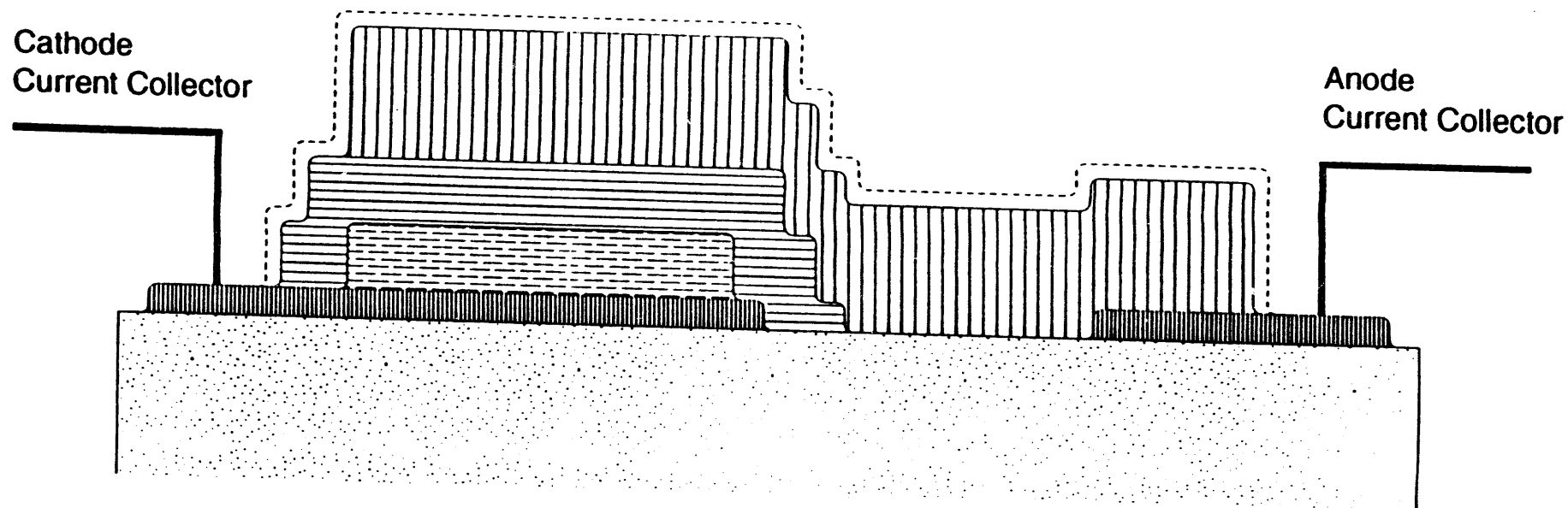
Cathode	Voltage (V)	Capacity	Energy Density <sup>a</sup> (Wh/l)	Specific Energy (Wh/kg)
		( $\mu\text{Ah}/\text{cm}^2\text{-}\mu\text{m}$ )		
TiS <sub>2</sub>	2.45-1.8	75	364	225
V <sub>2</sub> O <sub>5</sub>	3.7-1.5	123	611	444
Li <sub>x</sub> Mn <sub>2</sub> O <sub>4</sub>	4.2-4.0	40	433	211




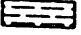

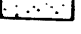
<sup>a</sup>Based on the combined mass of the lithium anode at three times overcapacity, the electrolyte film 1- $\mu\text{m}$  thick, and the cathode. Crystalline densities of the cathodes assumed to calculate the volume of the cells.

Figure Captions

- Fig. 1. Schematic cross section of a thin-film lithium battery.
- Fig. 2. Deposition sequence and typical geometry of a thin-film lithium battery.
- Fig. 3. (a) Examples of the first discharge to 2.7 V and first few cycles of a Li-V<sub>2</sub>O<sub>5</sub> cell. (b) Example of a discharge curve to 1.5 V.
- Fig. 4. The charge inserted into two V<sub>2</sub>O<sub>5</sub> cathodes as a function of the cycle number for cycling between 3.5 V and 1.5 V.
- Fig. 5. Discharge curves for a Li-V<sub>2</sub>O<sub>5</sub> cell for different current densities.
- Fig. 6. Impedance of two Li-V<sub>2</sub>O<sub>5</sub> cells at nearly full charge. The solid curves were obtained from a fit of the equivalent circuit model (see text) to the measured impedance.
- Fig. 7. Several charge-discharge curves for a Li-Li<sub>x</sub>Mn<sub>2</sub>O<sub>4</sub> cell following the initial charge. The current density was 30 μA/cm<sup>2</sup>.
- Fig. 8. The charge inserted into a Li<sub>x</sub>Mn<sub>2</sub>O<sub>4</sub> cathode as a function of the cycle number.
- Fig. 9. SEM micrograph of a fracture cross section of a Li-TiS<sub>2</sub> cell after more than 4000 cycles.

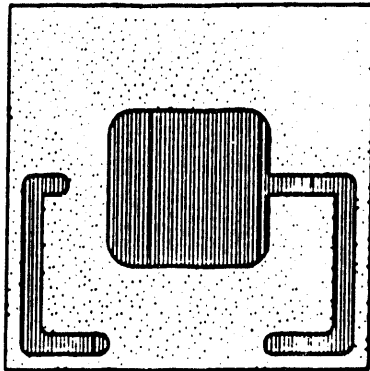
# Li / V<sub>2</sub>O<sub>5</sub> Rechargeable Thin-Film Battery



-  Protective Coating
-  Li
-  Li<sup>+</sup> electrolyte
-  V<sub>2</sub>O<sub>5</sub>
-  V
-  Substrate

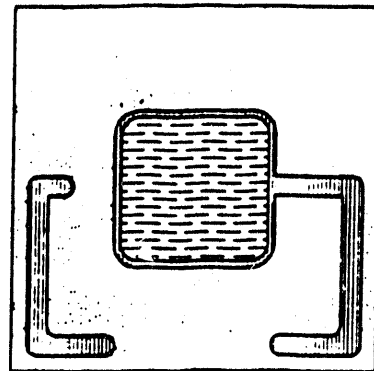
~ 2 μm

# Li / V<sub>2</sub>O<sub>5</sub> Rechargeable Thin-Film Battery



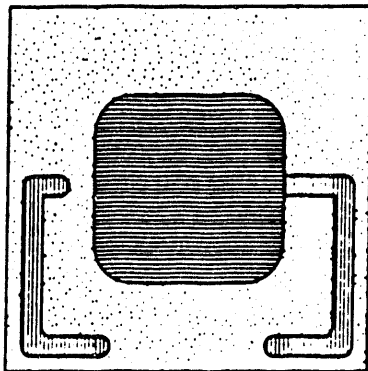
1

Vanadium geometry



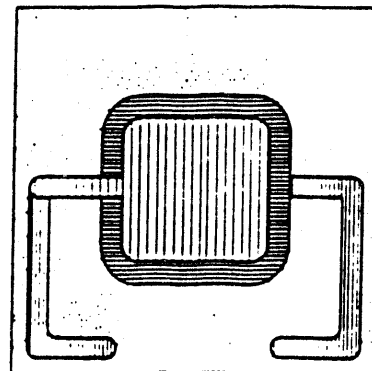
2

V<sub>2</sub>O<sub>5</sub> / V



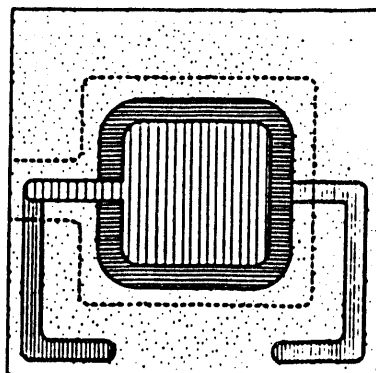
3

Li<sup>+</sup> electrolyte / V<sub>2</sub>O<sub>5</sub> / V



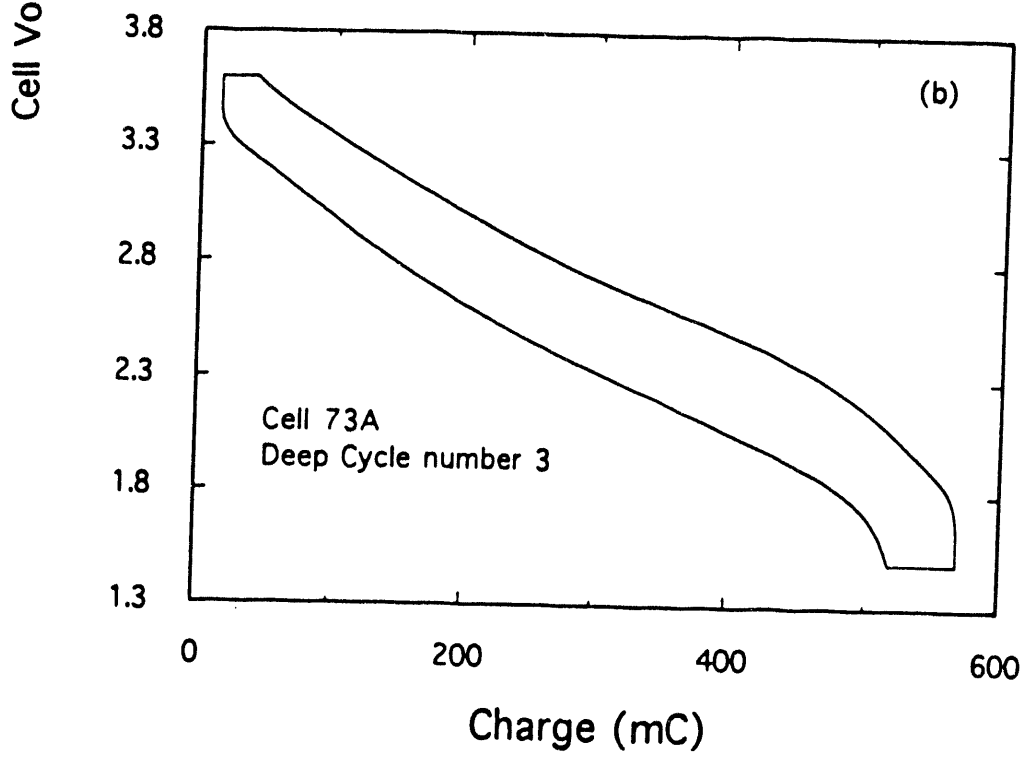
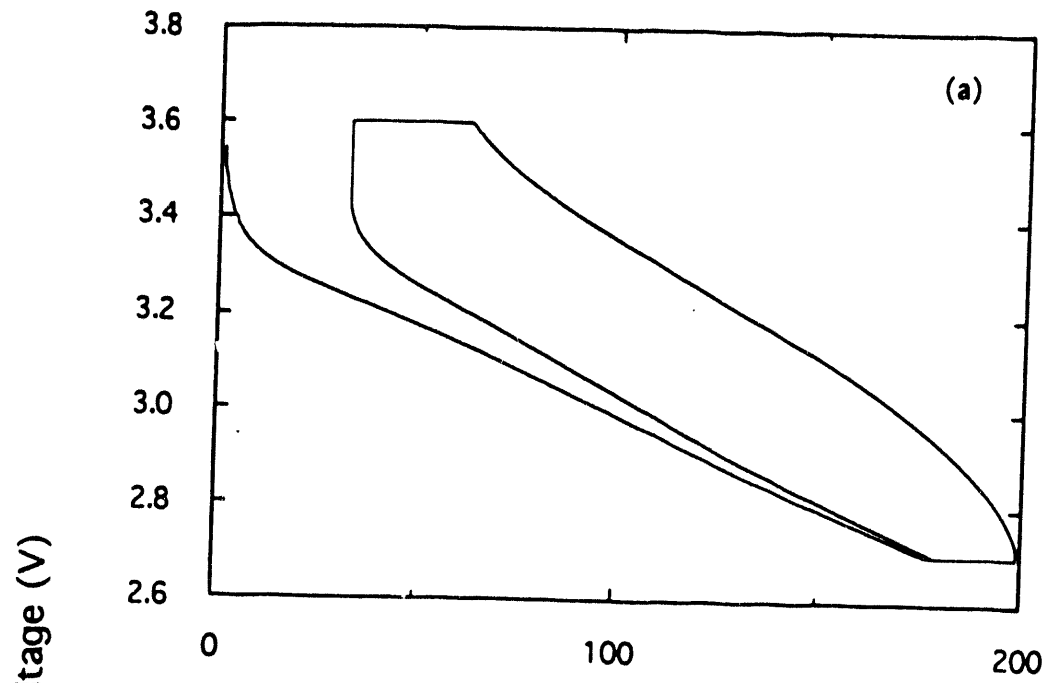
4

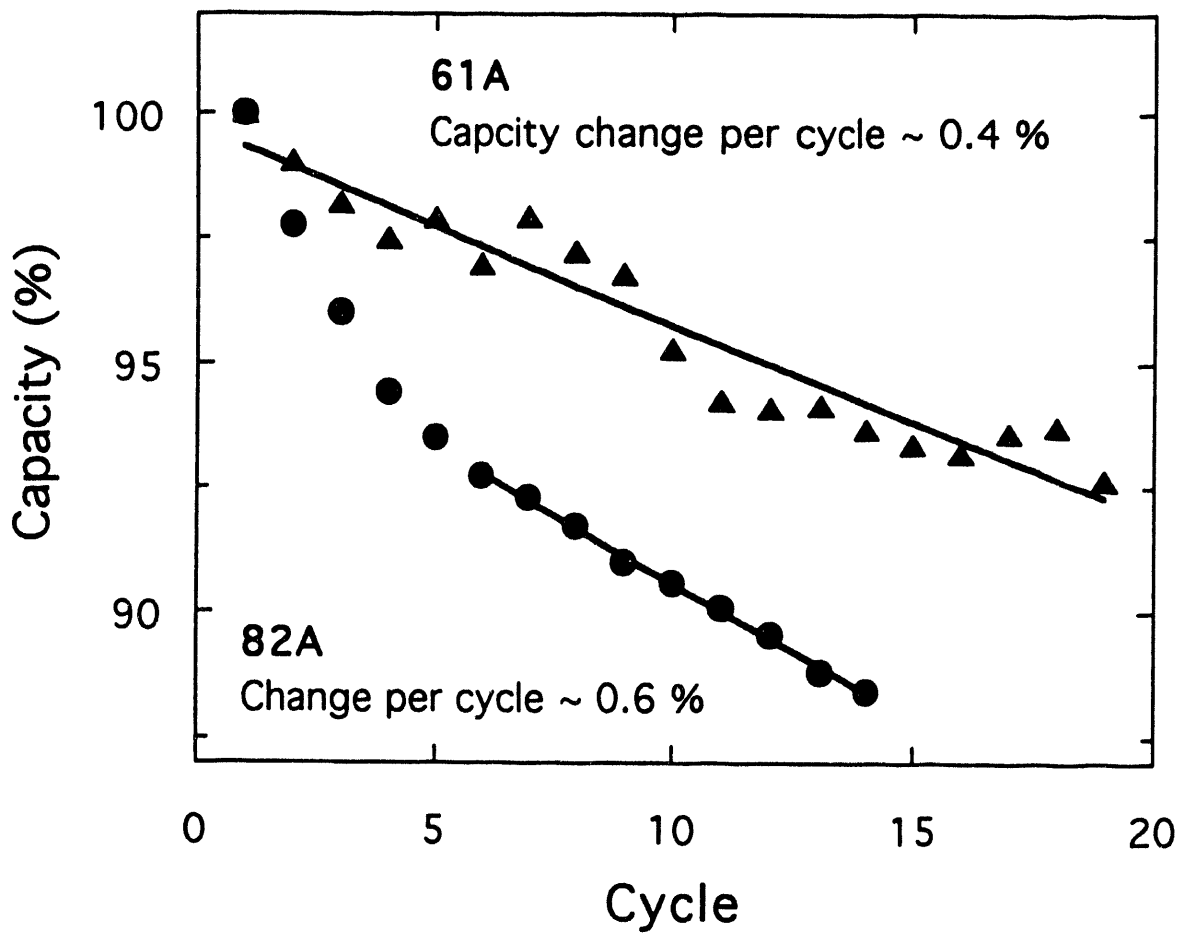
Li / Li<sup>+</sup> electrolyte / V<sub>2</sub>O<sub>5</sub> / V



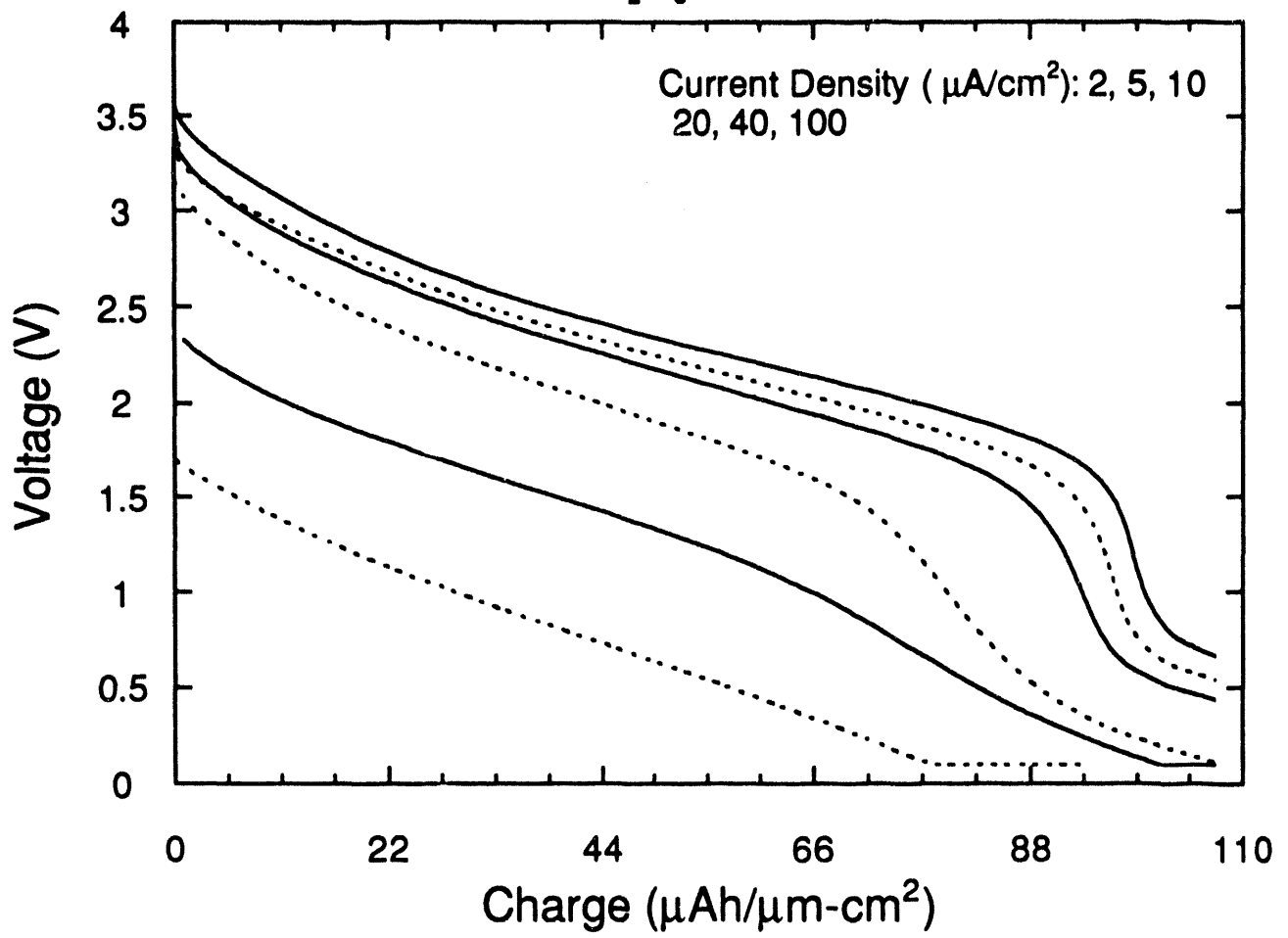
5

Protective Coating

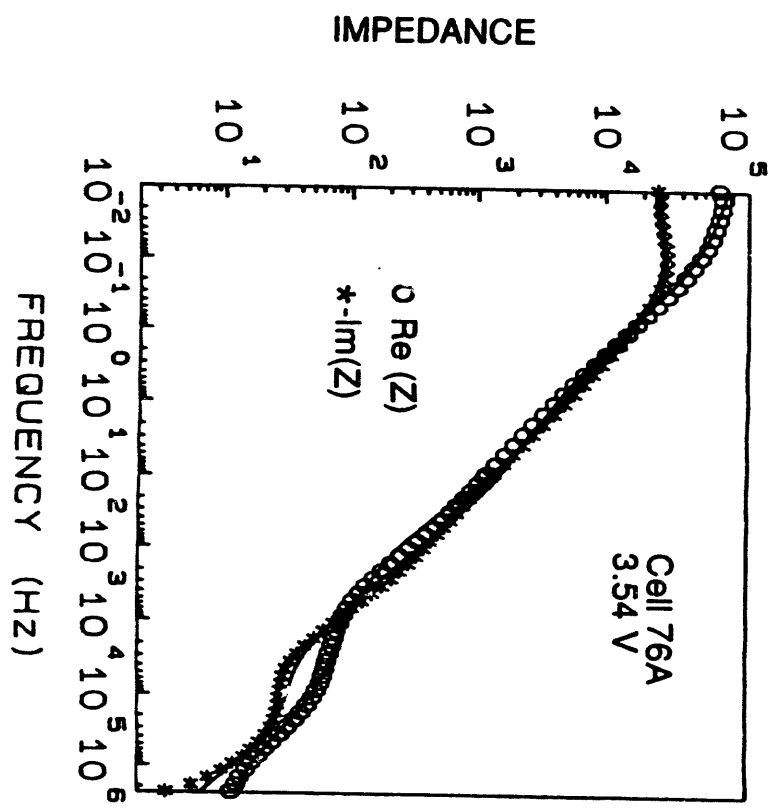
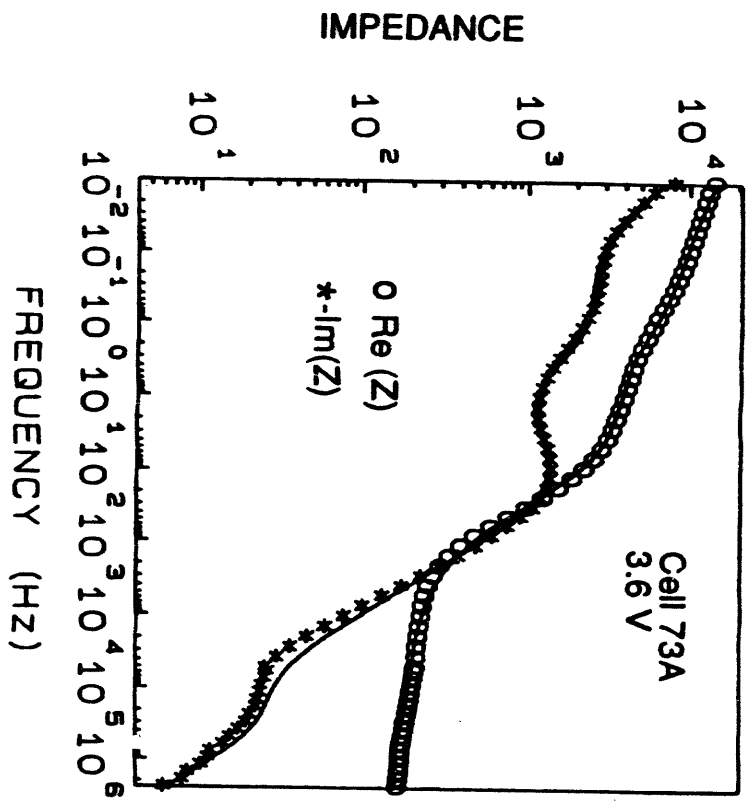


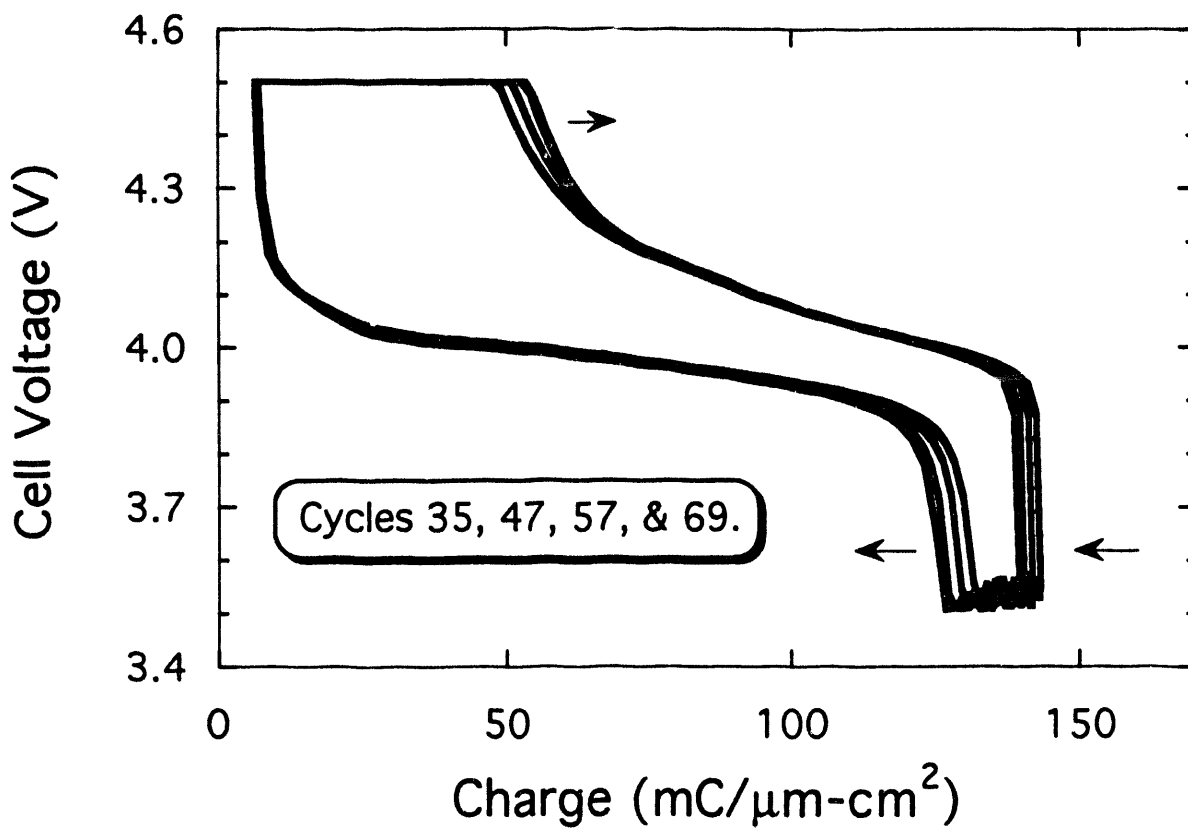


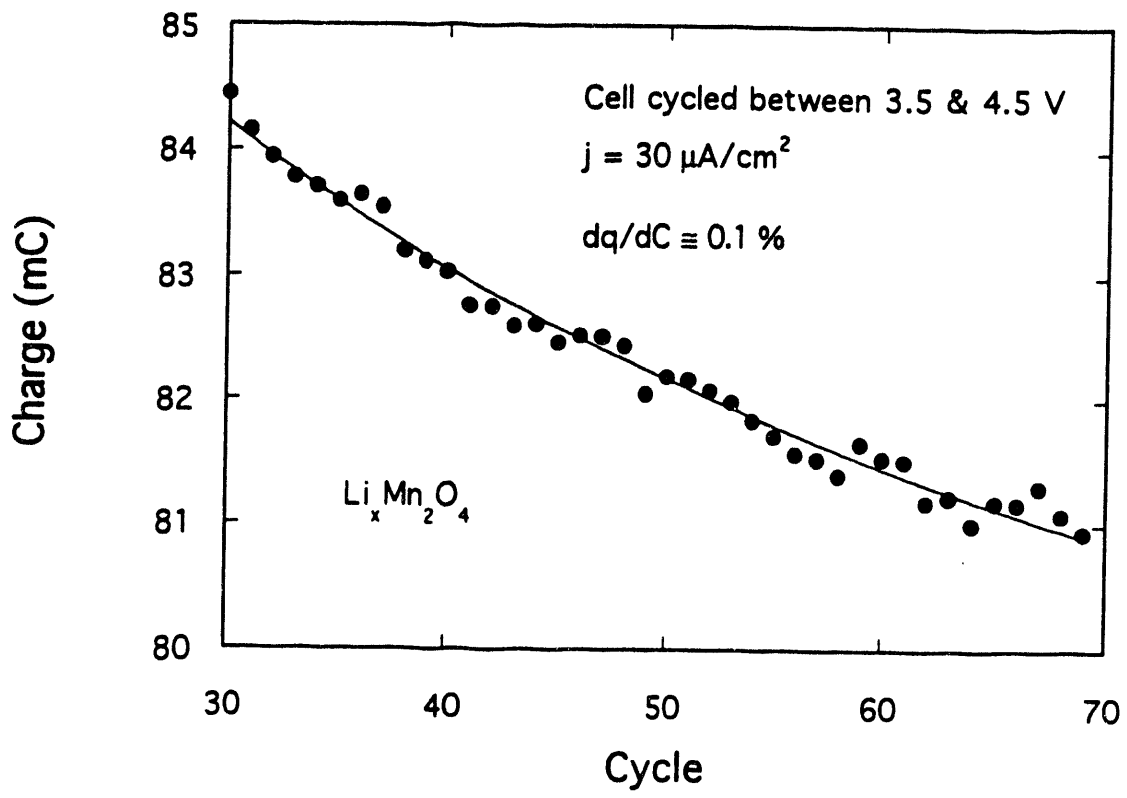
LI-V<sub>2</sub>O<sub>5</sub> Cell 83A



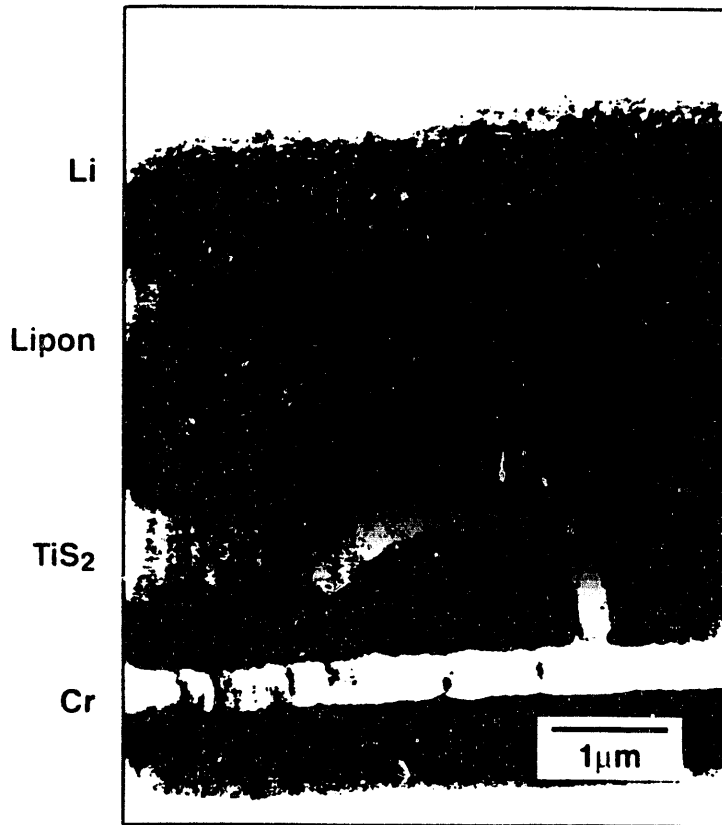








ORNL-DWG 93M-14782



**DATE  
FILMED**

*10/27/94*

**END**

